Effective field theory of cosmic acceleration: Constraining dark energy with CMB data

Marco Raveri,[1,2] Bin Hu,[3] Noemi Frusciante,[1,2] and Alessandra Silvestri[1,2,4]

[1]*SISSA-International School for Advanced Studies, Via Bonomea 265, 34136, Trieste, Italy*
[2]*INFN, Sezione di Trieste, Via Valerio 2, I-34127 Trieste, Italy*
[3]*Institute Lorentz, Leiden University, PO Box 9506, Leiden 2300 RA, The Netherlands*
[4]*INAF-Osservatorio Astronomico di Trieste, Via G.B. Tiepolo 11, I-34131 Trieste, Italy*

We introduce EFTCAMB/EFTCosmoMC as publicly available patches to the commonly used CAMB/CosmoMC codes. We briefly describe the structure of the codes, their applicability and main features. To illustrate the use of these patches, we obtain constraints on parametrized *pure* effective field theory and designer $f(R)$ models, both on ΛCDM and wCDM background expansion histories, using data from Planck temperature and lensing potential spectra, WMAP low-ℓ polarization spectra (WP), and baryon acoustic oscillations (BAO). Upon inspecting the theoretical stability of the models on the given background, we find nontrivial parameter spaces that we translate into *viability priors*. We use different combinations of data sets to show their individual effects on cosmological and model parameters. Our data analysis results show that, depending on the adopted data sets, in the wCDM background case these viability priors could dominate the marginalized posterior distributions. Interestingly, with Planck + WP + BAO + lensing data, in $f(R)$ gravity models, we get very strong constraints on the constant dark energy equation of state, $w_0 \in (-1, -0.9997)$ (95% C.L.).

I. INTRODUCTION

Ongoing and upcoming cosmological surveys will map matter and metric perturbations through different epochs with exquisite precision. Combined with geometric probes, they will provide us with a set of independent measurements of cosmological distances and the growth of structure. In the cosmological standard model, ΛCDM, the rate of linear clustering can be determined from the expansion rate of the Universe; however, this consistency relation is generically broken in models of modified gravity (MG) and dark energy (DE), even when they predict the same expansion history as ΛCDM. Therefore measurements of the growth of structure, such as weak lensing and galaxy clustering, add complementary constraining power to measurements of the expansion history via geometric probes. They can be used to perform consistency tests of ΛCDM and to constrain the parameter space of alternative approaches to the phenomenon of cosmic acceleration.

Over the past few years there has been a lot of activity in the community to construct frameworks [1–46] that would allow model-independent tests of gravity with cosmological surveys, like Planck [47], SDSS [48], DES [49], LSST [50], Euclid [51], WiggleZ Dark Energy Survey [52,53], and CFHTLenS [54–56]. These are generally based on parametrizations of the dynamics of linear scalar perturbations—either at the level of the equations of motion [39], of solutions of the equations [6,14,31], or of the action [57–59]—with the general aim of striking a delicate balance among the theoretical consistency, versatility, and feasibility of the parametrization. We shall focus on the latter approach,

in particular on the effective field theory (EFT) for cosmic acceleration developed in Refs. [57,58] (see Refs. [60–66] for previous work in the context of inflation, quintessence, and large-scale structure). This formalism relies on an action written in unitary gauge and built out of all the operators that are consistent with the unbroken symmetries of the theory, i.e., time-dependent spatial diffeomorphisms, and are ordered according to the power of perturbations and derivatives. At each order in perturbations, there is a finite number of such operators that enter the action multiplied by time-dependent coefficients commonly referred to as EFT functions. In particular, the background dynamics is determined solely in terms of the three EFT functions multiplying the three background operators, while the general dynamics of linear scalar perturbations is affected by further operators but can still be analyzed in terms of a handful of time-dependent functions. Despite the model-independent construction, there is a precise mapping that can be worked out between the EFT action and the action of any given single-scalar-field DE/MG model for which there exists a well-defined Jordan frame [57,58,67,68]. As such, the EFT of cosmic acceleration represents an insightful parametrization of the general quadratic action for single-scalar-field DE/MG which has the dual quality of offering a unified language to describe a broad range of single-field DE/MG models and a versatile framework for model-independent tests of gravity. For a more in-depth description of the EFT formalism we refer the reader to the original papers [57,58,69].

In Ref. [70] we introduced EFTCAMB, a patch which implements the effective field theory formalism of cosmic

acceleration into the public Einstein-Boltzmann solver CAMB [71,72]. As such, the code can be used to investigate the implications of the different EFT operators on linear perturbations as well as to study perturbations in any specific dark energy or modified gravity model that can be cast into the EFT language, once the mapping is worked out. Aside from its versatility, an important feature of EFTCAMB is that it evolves the full equations without relying on any quasistatic approximation and it still allows for the implementation of specific single-field models of DE/MG. Furthermore, as we will briefly review in Sec. II, our code has a built-in check of stability of the theory and allows one to safely evolve perturbations in models that cross the phantom divide.

We have now completed a modified version of the standard Markov Chain Monte Carlo (MCMC) code COSMOMC [73], which we dubbed EFTCOSMOMC. In combination with the check for stability of the theory embedded in EFTCAMB, it allows one to explore the parameter space of models of cosmic acceleration under general viability criteria that are well motivated from the theoretical point of view. It comes with built-in likelihoods for several cosmological data sets.

We illustrate the use of these patches to obtain constraints on different models within the EFT framework using data from Planck temperature and lensing potential spectra, WMAP low-ℓ polarization (WP) spectra, and baryon acoustic oscillations (BAO). In particular, we consider designer $f(R)$ models and an EFT linear parametrization involving only background operators on both a ΛCDM and wCDM bacgkround.

Finally, we are publicly releasing the EFTCAMB and EFTCOSMOMC patches at http://www.lorentz.leidenuniv.nl/hu/codes/. We are completing a set of notes that will guide the reader through the structure of the codes [74].

II. EFTCAMB

In this section we shall briefly review the main features of EFTCAMB. For a more in depth description of the EFT formalism, the equations evolved by the code, and the integration strategy, we refer the reader to Ref. [70].

The EFT formalism for cosmic acceleration is based on the following action written in unitary gauge and Jordan frame:

$$
\begin{aligned}
S = \int d^4x \sqrt{-g} &\Bigg\{ \frac{m_0^2}{2}(1+\Omega)R + \Lambda - a^2 c \delta g^{00} \\
&+ \frac{M_2^4}{2}(a^2 \delta g^{00})^2 - \frac{\bar{M}_1^3}{2}a^2 \delta g^{00} \delta K_\mu^\mu - \frac{\bar{M}_2^2}{2}(\delta K_\mu^\mu)^2 \\
&- \frac{\bar{M}_3^2}{2}\delta K_\nu^\mu \delta K_\mu^\nu + \frac{a^2 \hat{M}^2}{2}\delta g^{00}\delta R^{(3)} \\
&+ m_2^2(g^{\mu\nu}+n^\mu n^\nu)\partial_\mu(a^2 g^{00})\partial_\nu(a^2 g^{00}) + \cdots \Bigg\} \\
&+ S_m[\chi_i, g_{\mu\nu}],
\end{aligned}
\tag{1}
$$

where we have used conformal time and $\{\Omega, \Lambda, c, M_2, \bar{M}_1, \bar{M}_2, \bar{M}_3, \hat{M}, m_2\}$ are free functions of time which multiply all the operators that are consistent with time-dependent spatial diffeomorphism invariance and are at most quadratic in the perturbations. We will refer to these as EFT functions. The first line of Eq. (1) displays only operators that contribute to the evolution of the background. There follow the second-order operators that affect only the dynamics of perturbations, in combination with the background operators. The ellipses indicate higher-order operators which would affect the nonlinear dynamics and are not yet included in the code. Finally, S_m is the action for all matter fields, χ_i.

A given single-scalar-field model of DE/MG, for which there exists a well-defined Jordan frame, can be mapped into the formalism (1) as illustrated in Refs. [57,58,67,68]. As such, EFT offers a unified language for most of the viable approaches to cosmic acceleration; among others, we shall mention the Horndeski class [75] which includes quintessence [76], k-essence [77], $f(R)$, the covariant Galileon [78], and the effective four-dimensional limit of Dvali-Gabadadze-Porrati gravity [79]. Furthermore, the action (1) represents a parametrized framework to test gravity on large scales via the dynamics of linear cosmological perturbations. To this extent, one can use a designer approach to fix *a priori* the background evolution and use the Friedmann equations to determine two of the EFT background functions $\{\Omega, \Lambda, c\}$ in terms of the third one [57,58]. It turns out to be convenient to solve for c and Λ in terms of Ω. In the unitary gauge adopted for the action (1), the extra scalar d.o.f. associated to DE or the modifications of gravity is eaten by the metric. While such set up is convenient to construct the action, in order to analyze the dynamics of perturbations it is convenient to make the scalar d.o.f. explicit. This can be achieved restoring the time-diffeomorphism invariance of the action via the Stückelberg technique, i.e., performing an infinitesimal time diffeomorphism transformation to the action,

$$
\tau \to \tau + \pi(x^\mu),
\tag{2}
$$

and Taylor expanding the resulting action in π. The Stückelberg field, π, now encodes the departures from the standard cosmological model. At the level of linear scalar perturbations, EFTCAMB evolves the standard equations for all matter species, a set of modified Einstein-Boltzmann equations, and a full Klein-Gordon equation for π, as described at length in Ref. [70]. We shall recall that this treatment of the extra dynamics associated to DE/MG—as opposed to an effective fluid approach [27,80,81]—allows us to maintain better control over the stability of the theory and to cross the phantom divide.

As described in Ref. [70], the multifaceted nature of the EFT formalism is implemented in EFTCAMB, where the background dynamics can be approached with either of the following procedures:

(i) Pure EFT: In this case one works with a given subset of the operators in Eq. (1) (possibly all of them), treating their coefficients as free functions. The background is treated via the EFT designer approach, i.e., a given expansion history is fixed, a viable form for Ω [82] is chosen, and the remaining two background EFT functions are determined via the Friedmann equations. The code allows for ΛCDM and wCDM expansion histories, as well as for the Chevallier-Polarski-Linder (CPL) [83,84] parametrization of the dark energy equation of state. In addition, it offers a selection of functional forms for $\Omega(a)$: the minimal coupling, corresponding to $\Omega = 0$; the linear model, which can be thought of as a first-order approximation of a Taylor expansion; a power law, inspired by $f(R)$; and exponential forms. There is also the possibility for the user to choose an arbitrary form of Ω according to any *ansätz* the user wants to investigate. At the level of perturbations, more operators come into play, each with a free function of time in front of it, and one needs to choose some *ansätze* in order to fix their functional form. To this extent, we adopted the same scheme as for the background function Ω, which still provides the possibility of defining and using other forms that might be of interest. Of course the possibility to set all/some second-order EFT functions to zero is included. The code evolves the full perturbed equations consistently, and the implementation accounts for the inclusion of more than one second-order operator per time, ensuring that even more and more complicated models can be studied.

(ii) Mapping EFT: In this case a particular DE/MG model is chosen, the corresponding background equations are solved, and then everything is mapped into the EFT formalism [57,58,67,68] to evolve the full EFT perturbed equations. Let us stress that in the mapping case, once the background equations are solved, all the EFT functions are completely fixed by the choice of the model. Built in to the first code release are $f(R)$ models for which a designer approach is used for the ΛCDM, wCDM, and CPL backgrounds following Refs. [85,86]. In the future other theories will be added to gradually cover the wide range of models included in the EFT framework.

In summary, EFTCAMB is a full Einstein-Bolztmann code which exploits the double nature of the EFT framework. As such, it allows one to investigate how the different operators entering Eq. (1) affect the dynamics of linear perturbations and to study a particular DE/MG model, once the mapping to the EFT formalism is determined. Let us stress that EFTCAMB evolves the full dynamical equations on all linear scales in both the pure EFT and mapping modes, ensuring that we do not miss out on any potentially interesting dynamics at redshifts and scales that might be within reach of upcoming, wider and deeper surveys.

Ultimately, we built a machinery which allows one to test gravity and its modifications on large scales in a model-independent framework which ideally covers most of the models of cosmological interest by computing cosmological observables which are the two-point auto- and cross-correlations provided by the combination of galaxy clustering, CMB temperature, polarization anisotropy, and weak lensing data.

III. EFTCOSMOMC: SAMPLING OF THE PARAMETER SPACE UNDER STABILITY CONDITIONS

To fully exploit the power of EFTCAMB we equipped it with a modified version of the standard Markov Chain Monte Carlo code COSMOMC [73], which we dubbed EFTCOSMOMC. The complete code now allows one to explore the parameter space performing comparisons with several cosmological data sets, and it does so with a built-in stability check that we shall discuss in the following.

In the EFT framework, the stability of perturbations in the dark sector can be determined from the equation for the perturbation π, which is an inhomogeneous Klein-Gordon equation with coefficients that depend on both the background expansion history and the EFT functions [57,58,70]. Following the arguments of Ref. [61], in Ref. [70] we listed general viability requirements in the form of conditions to impose on the coefficients of the equation for π; these include a speed of sound $c_s^2 \leq 1$, a positive mass $m_\pi^2 \geq 0$, and the avoidance of ghost. Furthermore, we required a positive nonminimal coupling function, i.e., $1 + \Omega > 0$, to ensure a positive effective Newton constant.

When exploring the parameter space one needs to check the stability of the theory at every sampling point. While this feature at first might seem a drawback, it is actually one of the main advantages of the EFT framework and a virtue of EFTCAMB/EFTCOSMOMC. Indeed, as we outlined in Ref. [70], checking the stability of the theory ensures not only that the dynamical equations are mathematically consistent and can be reliably numerically solved, but also (perhaps more importantly) that the underlying physical theory is acceptable. This of course is desired when considering specific DE/MG models and, even more, when adopting the pure EFT approach. Indeed, in the latter case one makes a somewhat arbitrary choice for the functional form of the EFT functions, and satisfying the stability conditions will ensure that there is an underlying, theoretically consistent model of gravity corresponding to that given choice.

Imposing stability conditions generally results in a partition of the parameter space into a stable region and an unstable one. In order to not alter the statistical properties of the MCMC sampler [87] (such as the convergence to the target distribution), when dealing with a partitioned parameter space we implement the stability conditions as

priors so that the Monte Carlo step is rejected whenever it would fall in the unstable region. We call these constraints *viability priors* as they represent the degree of belief in a viable underlying single-scalar-field DE/MG theory encoded in the EFT framework. We would like to stress that they correspond to specific conditions that are theoretically well motivated, and hence they represent the natural requirements to impose on a model/parametrization. One of the virtues of the EFT framework, and consequently of EFTCAMB/EFTCoSMOMC, is to allow for their implementation in a straightforward way. We shall emphasize that our EFTCoSMOMC code automatically enforces the viability priors for every model considered, in both the pure and mapping EFT approaches.

IV. DATA SETS AND RESULTS

In this section we shall briefly review the data sets we used and discuss the resulting constraints obtained for some selected pure and mapping EFT models on both ΛCDM and wCDM backgrounds. While we will work with models that involve only background operators, EFTCAMB/ EFTCoSMOMC is fully equipped to also handle second-order operators; the same procedure that we shall outline here can be followed when the latter are used.

A. Data sets

We adopt Planck temperature-temperature power spectra, considering the nine frequency channels ranging from 30–353 GHz for low-ℓ modes ($2 \leq \ell < 50$) and the 100, 143, and 217 GHz frequency channels for high-ℓ modes ($50 \leq \ell \leq 2500$)[1] [88,89]. In addition, we include the Planck Collaboration's 2013 data release of the full-sky lensing potential map [90], by using the 100, 143, and 217 GHz frequency bands with an overall significance greater than 25σ. The lensing potential distribution is an indicator of the underlying large-scale structure, and as such it is sensitive to the modified growth of perturbations contributing significant constraining power for DE/MG models.

In order to break the well-known degeneracy between the reionization optical depth and the amplitude of cosmic microwave background (CMB) temperature anisotropy, we include WMAP low-ℓ polarization spectra ($2 \leq \ell \leq 32$) [91]. Finally, we consider the external baryon acoustic oscillations measurements from the 6dFGS ($z = 0.1$) [92], SDSS DR7 (at effective redshift $z_{\text{eff}} = 0.35$) [93,94], and BOSS DR9 ($z_{\text{eff}} = 0.2$ and $z_{\text{eff}} = 0.35$) [95] surveys to get complementary constraining power on cosmological distances.

To explicitly show the effect of individual data sets on the different parameters that we constrain, we adopt three different combinations of data: Planck + WP,

Planck + WP + BAO, and Planck + WP + BAO + lensing, where by "lensing" we mean the CMB lensing potential distributions as measured by Planck. In all cases we assume standard flat priors from CMB on cosmological parameters while we impose the viability priors discussed in Sec. III on model parameters.

B. Linear EFT model

We start our exploration of CMB constraints on DE/MG theories with a pure EFT model. We adopt the designer approach choosing two different models for the expansion history: the ΛCDM one and the wCDM one (corresponding to a constant dark energy equation of state). As we reviewed in Sec. II, after fixing the background expansion history one can use the Friedmann equations to solve for two of the three EFT background functions in terms of the third one; as is common, we use this to eliminate Λ and c. We are then left with Ω as a free background function that will leave an imprint only on the behavior of perturbations. We assume the following functional form:

$$\Omega(a) = \Omega_0^{\text{EFT}} a, \qquad (3)$$

which can be thought of as a first-order approximation of a Taylor expansion in the scale factor. We set to zero the coefficients of all the second-order EFT operators. In the remaining we refer to this model as the linear EFT model.

Before proceeding with parameter estimation, it is instructive to study the shape of the viable region in the parameter space of the model. As we discussed in Sec. III, the check on the stability of any given model is a built-in feature of EFTCAMB/EFTCoSMOMC, so that the user does not need to separately perform such an investigation prior to implementing the model in the code. Nevertheless, in some cases it might be useful to look at the outcome of such an analysis, as one can learn interesting things about the model/parametrization under consideration. Let us briefly discuss the stability of the linear EFT model.

In the case of a ΛCDM expansion history, it is easy to show that all the stability requirements that we listed in Ref. [70], and reviewed in Sec. III, imply the following viability prior:

$$\Omega_0^{\text{EFT}} \geq 0. \qquad (4)$$

On the other hand, the case of a wCDM expansion history cannot be treated analytically so we used our EFTCAMB code along with a simple sampling algorithm, included in the code release, to explore the stability of the model in the parameter space. We varied the parameters describing the dark-sector physics while keeping fixed all the other cosmological parameters. The result is shown in Fig. 1 and includes interesting information on the behavior of this model. First of all, also in this case the stable region corresponds to $\Omega_0^{\text{EFT}} > 0$; furthermore, it is possible to have

---

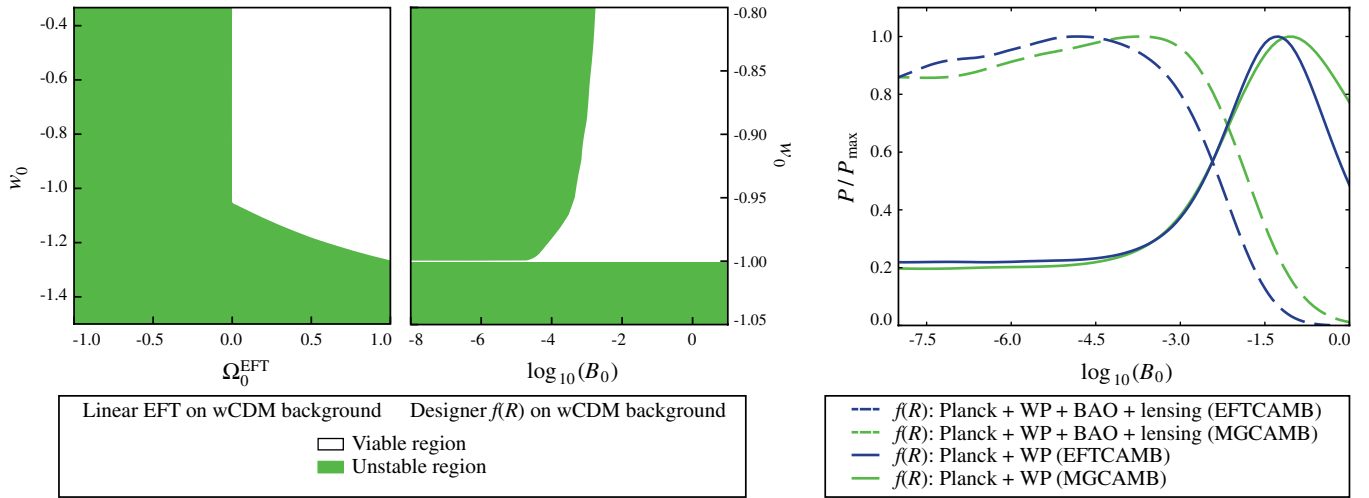[1]http://pla.esac.esa.int/pla/aio/planckProducts.html.

FIG. 1 (color online).   Left panel: Stability regions of linear EFT and designer $f(R)$ models on a wCDM background. The cosmological parameters defining the expansion history are set to their CAMB default values: $H_0 = 70$ Km/s/Mpc, $\Omega_b = 0.05$, $\Omega_c = 0.22$, and $T_{\text{CMB}} = 2.7255$ K. Right panel: Marginalized constraints on $\log_{10}(B_0)$ describing designer $f(R)$ models on a ΛCDM background for two data sets differing by CMB lensing and BAO. For each data set we compare the results obtained with EFTCAMB with those obtained by MGCAMB [102,103] for the same designer $f(R)$ models.

a viable gravity model with $w_0 < -1$, although in this case Ω_0^{EFT} needs to acquire a bigger and bigger value to stabilize perturbations in the dark sector. Finally, we see that if $\Omega_0^{\text{EFT}} = 0$ we recover the result—found in the context of quintessence models [96]—that $w_0 > -1$. This case corresponds, in fact, to minimally coupled quintessence models with a potential that is crafted so that the resulting expansion history mimics that of a wCDM model.

For the ΛCDM background case, the one-dimensional marginalized posterior distributions, obtained with the three different data compilations discussed above, are shown in Fig. 3(a). The corresponding marginalized statistics are summarized in Table I(a). We find that the three different data compilations produce similar results, with Planck + WP + BAO + lensing giving

$$\Omega_0^{\text{EFT}} < 0.061 \quad (95\% \text{ C.L.}). \qquad (5)$$

Next we consider a wCDM expansion history, characterized by an equation of state for dark energy that is constant in time, w_0, but different from -1. Upon inspecting Fig. 3(b) one can notice that the marginalized posterior distributions of $(\Omega_m, \Omega_\Lambda, H_0, w_0)$ obtained from Planck + WP data are significantly skewed, i.e., their right tail goes to zero much more sharply than the left one. The situation changes significantly when one adds BAO data. This is due to the combination of two effects. On the one hand, when BAO data are not included, the constraints on $(\Omega_m, \Omega_\Lambda, H_0, w_0)$ are relatively loose since one is lacking the complementary high-precision information on the expansion history. In other words, the gain/loss of the likelihood value in the vicinity of best-fit points is not very significant, so the sampling points of cosmological parameters broadly spread around their central values.

In this case, the stability requirements on Ω_0^{EFT} and w_0 dominate over the data-constraining power. On the other hand, as shown in the left panel of Fig. 1, the viable region in the space $(\Omega_0^{\text{EFT}}, w_0)$ for the linear EFT model on a wCDM background covers mostly $w_0 > -1$, i.e., it is highly asymmetric in the range around $w_0 = -1$. This explains the asymmetry in the posterior distribution of w_0 since the marginalized posterior distribution in Monte Carlo integration algorithms follows the number of projected sampling points in the given volume. Furthermore, from Fig. 2(a) (green curve), one can see that $(\Omega_m, \Omega_0^{\text{EFT}}, H_0)$ are degenerate (as expected) with w_0, and this explains why their posterior distributions are skewed as well. As soon as complementary measurements of cosmological distances (such as BAO) are added to the data sets, the constraining power is strong enough and the posterior distributions become more symmetric; indeed, BAO data significantly helps to localize the confidence regions close to $w_0 \sim -1$, making the posterior distribution less affected by the global profile of viability priors.

Finally, from Fig. 2(a) we can see that the degeneracy of Ω_0^{EFT} with the other parameters is not very significant after adding BAO data (blue and red curves). As a result the bounds on Ω_0^{EFT} remain at the same level as those obtained for a ΛCDM background. With Planck + WP + BAO + lensing data we obtain

$$\Omega_0^{\text{EFT}} < 0.058 \quad (95\% \text{ C.L.}). \qquad (6)$$

One can notice that the addition of lensing data does not significantly improve the constraint on Ω_0^{EFT} in either the ΛCDM or the wCDM case.
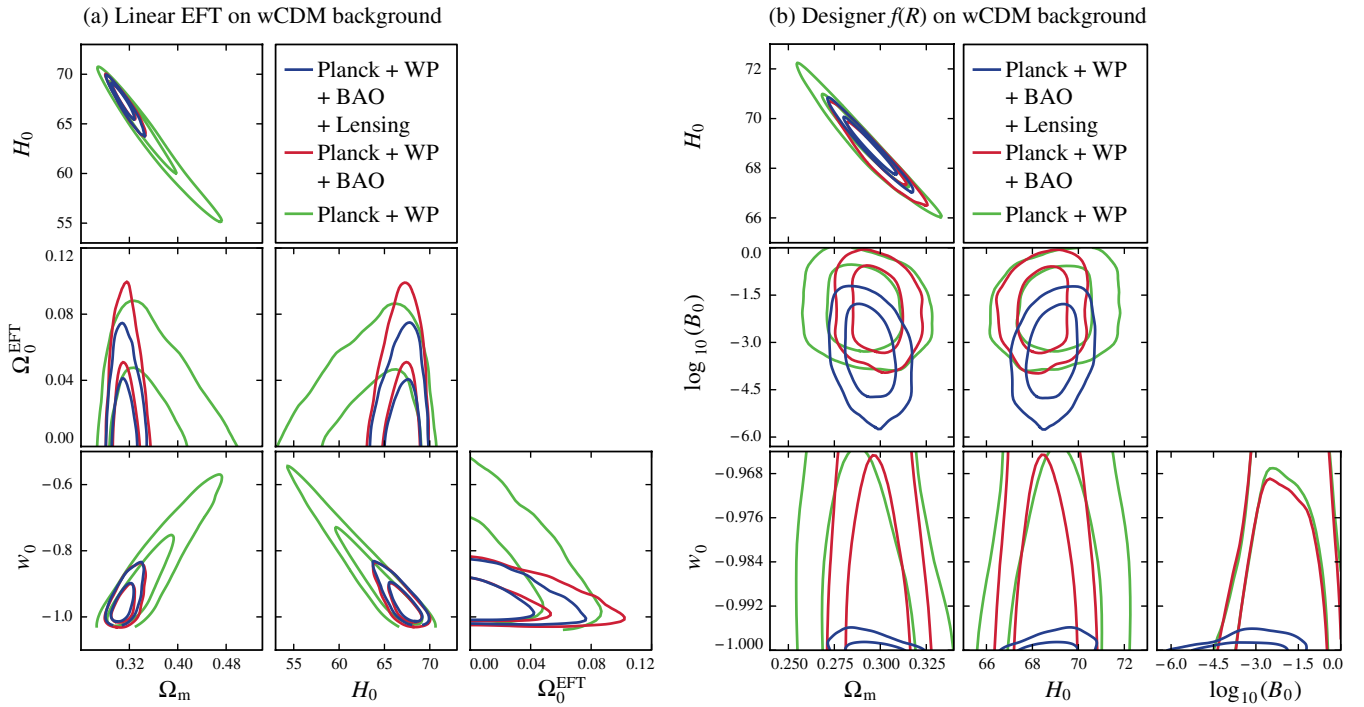
FIG. 2 (color online).   68% and 95% confidence regions on combinations of cosmological parameters for linear pure EFT and designer $f(R)$ models on a wCDM background. Different combinations of observables are indicated with different colors.

C. $f(R)$ gravity

The simplicity of its theoretical structure and the representative phenomena to which it leads at the level of growth of structure have long made $f(R)$ gravity a popular model of modified gravity. We refer the reader to Refs. [85,86,97,98] for detailed discussions of the cosmology of $f(R)$ models. Here we shall briefly review the main features that are of interest for our analysis.

We consider the following action in Jordan frame:

$$S = \int d^4x \sqrt{-g}[R + f(R)] + S_m, \qquad (7)$$

where $f(R)$ is a generic function of the Ricci scalar and the matter sector is minimally coupled to gravity. The higher-order nature of the theory translates into having an extra scalar d.o.f. which can be identified with $f_R \equiv df/dR$, commonly dubbed the scalaron [99]. As explained in Ref. [57], these models can be mapped into the EFT formalism via the following matching:

$$\Lambda = \frac{m_0^2}{2}[f - Rf_R]; \quad c = 0; \quad \Omega = f_R. \qquad (8)$$

Within the EFT language, the role of the perturbation to the scalaron, δf_R, is played by the Stückelberg field which, in the $f(R)$ case, corresponds to $\pi = \delta R/R$ [57].

It is well known that given the higher order of the theory, it is possible to reproduce any given expansion history by

an appropriate choice of the $f(R)$ function [85,86]. In other words, $f(R)$ models can be treated with the so-called *designer* approach, which consists in fixing the expansion history and then using the Friedmann equation as a second-order differential equation for $f[R(a)]$. Generically, one finds a family of viable models that reproduce the given expansion; the latter are commonly labeled by the boundary condition at present time, f_R^0. Equivalently, they can be parametrized by the present value, B_0, of the Compton wavelength of the scalaron in Hubble units,

$$B = \frac{f_{RR}}{1 + f_R} \frac{\mathcal{H}\dot{R}}{\dot{\mathcal{H}} - \mathcal{H}^2}, \qquad (9)$$

where dots indicate derivatives with respect to conformal time. B_0 can be related to f_R^0 and one approximately has $B_0 \approx -6f_R^0$ in the ΛCDM case. Let us recall that the heavier the scalaron, the smaller B_0 and $|f_R^0|$.

Finally, as discussed in Refs. [85,86,100,101], $f(R)$ models need to satisfy certain conditions of stability and consistency with local tests of gravity [86]; the latter can be inferred from the conditions discussed in Sec. III once the matching (8) is implemented.

As described at length in our previous work [70], EFTCAMB treats the background of $f(R)$ gravity with a built-in designer routine that is specific to these models and can handle ΛCDM, wCDM, and CPL backgrounds. Furthermore, the viability of the reconstructed model is

automatically checked by the code via the procedure described in Sec. III.

Like in the pure EFT case, it proves very instructive to investigate the shape of the parameter space as dictated by the stability conditions of Sec. III. For the designer $f(R)$ model on a ΛCDM background it is easy to show that the latter reproduce the known result that in order to have a positive mass of the scalaron, B_0 should be greater than zero. It is much more interesting to investigate the shape of the parameter space for $f(R)$ models mimicking a wCDM background expansion history. We do it numerically, through the built-in routine of EFTCAMB, and we show the results in Fig. 1. The first noticeable feature is that for wCDM models the value of the equation of state of dark energy cannot go below -1, which is consistent with what was found in Ref. [86]. The second is that the parameter B_0 controls the limit to General Relativity (GR) of the theory, i.e., when B_0 gets smaller the expansion history is forced to go back to that of the ΛCDM model in order to preserve a positive mass of the scalaron. The converse is not true and this same feature do not appear in pure EFT models where the $\Omega_0^{\mathrm{EFT}} = 0$ branch contains viable theories and corresponds to the wide class of minimally coupled quintessence models.

In what follows, we shall first investigate the constraints on B_0 in models reproducing the ΛCDM background, performing also a comparison with analogous results obtained using MGCAMB [102,103]. We will then move to study constraints on designer models on a wCDM background, which is a novel aspect of our work.

In the right panel of Fig. 1, we compare the one-dimensional marginalized posterior distributions of $\log_{10} B_0$ from our EFTCAMB to those from MGCAMB. Overall there is good agreement between the two results. Moreover, one can notice that generally the constraints obtained with EFTCAMB are a little bit tighter than those obtained with MGCAMB. This is because in the latter code $f(R)$ models are treated with the quasistatic approximation which loses out on some of the dynamics of the scalaron [104], which is instead fully captured by our full Einstein-Boltzmann solver, as discussed already in Ref. [70].

The detailed one-dimensional posterior distributions and corresponding marginalized statistics are summarized in Fig. 3(c) and Table I(b) and they are consistent with previous studies employing the quasistatic approximations [105]. The right panel of Fig. 1 and Fig. 3(c) show that lensing data add a significant constraining power on B_0. This is because Planck lensing data are helpful in breaking the degeneracy between Ω_m and B_0, which affect the lensing spectrum in different ways. Indeed, in $f(R)$ gravity the growth rate of linear structure is enhanced by the modifications, and hence the amplitude of the lensing potential spectrum is amplified whenever B_0 is different than zero (see our previous work [70]); however, the background angular diameter distance is not affected by

B_0, so the position of the lensing potential spectrum is not shifted horizontally. On the other hand, Ω_m affects both the background and linear perturbation so that both the amplitude and position of the peaks of the lensing potential are sensitive to it.

Similarly to what happens in the linear EFT model, $f(R)$ gravity shows some novel features in the case of a wCDM background. Once again we find a nontrivial likelihood profile of $\log_{10} B_0$ [see Fig. 3(d)] for all three data compilations, with the shape of the marginalized posterior distribution of $\log_{10} B_0$ being dominated by the shape of the stable region. In the middle panel of Fig. 1 one can see indeed that when B_0 tends to smaller values, i.e., the theory tends to GR, the stable regions becomes narrower and narrower, with a tiny tip pointing to the GR limit. Since the width of this tip is so narrow compared with the current capability of parameter estimation from Planck data, the gains of likelihood of the sampling points inside this parameter throat are not significant, i.e., they are uniformly sampled in the throat. Hence, even though the full data set has a very good sensitivity to B_0, the marginalized distribution of $\log_{10} B_0$ is dominated by the volume of the stable region in the parameter space. A complementary consequence of the shape of the stable region in the (B_0, w_0) space is the fact that when B_0 tends to zero, w_0 is driven to -1. In other words, the stability conditions induce a strong correlation between B_0 and w_0 and, as a consequence, in $f(R)$ models—on either a ΛCDM or wCDM background—the GR limit is effectively controlled by a single parameter, i.e., B_0.

Finally, one can notice that the bound on w_0 with Planck lensing data is quite stringent compared to those without lensing:

$$w_0 \in (-1, -0.94) \ (95\% \ \mathrm{C.L.}) \ \mathrm{without\, lensing},$$

$$w_0 \in (-1, -0.9997) \ (95\% \ \mathrm{C.L.}) \ \mathrm{with\, lensing}. \qquad (10)$$

We argue that this stringent constraint is actually a consequence of the combination of the strong correlation between B_0 and w_0 induced by the viability prior (as discussed above) and the sensitivity of lensing data to B_0, which we capture well with our code. As shown in Ref. [34], Planck lensing data is very sensitive to MG parameters such as B_0; indeed, in our analysis with Planck + WP + BAO + lensing data we get

$$\log_{10} B_0 = -3.35^{+1.79}_{-1.77} \quad (95\% \ \mathrm{C.L.}). \qquad (11)$$

Furthermore, from Fig. 2(b) one can see that the ellipse in the $(\log_{10} B_0, w_0)$ space corresponding to Planck + WP + BAO + lensing data (blue) is orthogonal to those without lensing (red and green). In other words, when lensing data is included, $\log_{10} B_0$ and w_0 display a degeneracy which propagates the stringent constraint on the scalar Compton wavelength from CMB lensing data to w_0. Besides this, we
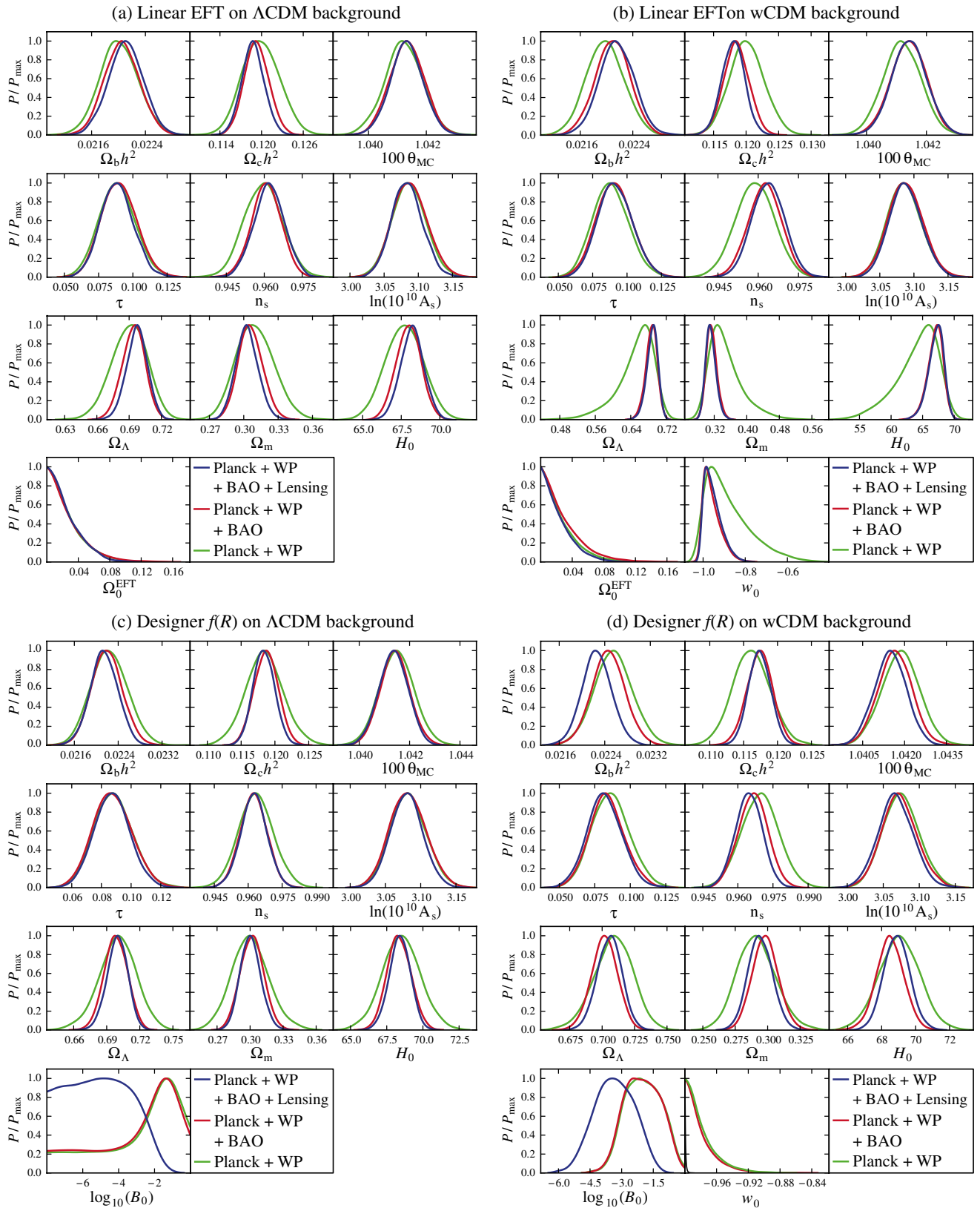
FIG. 3 (color online).   One-dimensinoal marginalized posterior distributions of cosmological and model parameters for pure linear EFT (a,b) and $f(R)$ (c,d) models on both ΛCDM (a,c) and wCDM (b,d) backgrounds. Different colors represent different combinations of cosmological data sets.

TABLE I.   Constraints on cosmological parameters, using different combinations of CMB data sets, of linear pure EFT (a) and designer $f(R)$ (b) models, on both ΛCDM (left) and wCDM (right) backgrounds.

(a) Mean values and 68% (or 95%) confidence limits for primary/derived parameters for a linear EFT model on a ΛCDM/wCDM background

	Linear EFT $+ \Lambda$CDM			Linear EFT $+ w$CDM		
	Planck $+$ WP	Planck $+$ WP $+$ BAO	Planck $+$ WP$+$ BAO $+$ lensing	Planck $+$ WP	Planck $+$ WP $+$ BAO	Planck $+$ WP$+$ BAO $+$ lensing
Parameters	mean $\pm$68% C.L.	mean $\pm$68% C.L.	mean $\pm$68% C.L.	mean $\pm$68% C.L.	mean $\pm$68% C.L.	mean $\pm$68% C.L.
$100\Omega_b h^2$	2.201 ± 0.028	2.205 ± 0.025	2.211 ± 0.025	2.198 ± 0.028	2.209 ± 0.026	2.216 ± 0.026
$\Omega_c h^2$	0.1199 ± 0.0026	0.1193 ± 0.0017	0.1188 ± 0.0016	0.1201 ± 0.0026	0.1185 ± 0.0019	0.1180 ± 0.0018
$100\theta_{MC}$	1.04121 ± 0.00063	1.04133 ± 0.00058	1.04132 ± 0.00055	1.04119 ± 0.00062	1.04141 ± 0.00058	1.04142 ± 0.00058
τ	0.089 ± 0.013	0.090 ± 0.013	0.088 ± 0.012	0.088 ± 0.013	0.091 ± 0.013	0.091 ± 0.012
n_s	0.9596 ± 0.0073	0.9608 ± 0.0057	0.9619 ± 0.0059	0.9588 ± 0.0071	0.9625 ± 0.0060	0.9637 ± 0.0060
$\log(10^{10}A_s)$	3.086 ± 0.024	3.088 ± 0.025	3.084 ± 0.022	3.086 ± 0.025	3.088 ± 0.025	3.088 ± 0.023
Ω_0^{EFT}	< 0.066 (95% C.L.)	< 0.072 (95% C.L.)	< 0.061 (95% C.L.)	< 0.065 (95% C.L.)	< 0.076 (95% C.L.)	< 0.058 (95% C.L.)
w_0	$\cdots$	$\cdots$	$\cdots$	$-0.88^{+0.21}_{-0.14}$ (95% C.L.)	$-0.96^{+0.09}_{-0.06}$ (95% C.L.)	$-0.95^{+0.08}_{-0.07}$ (95% C.L.)
Ω_m	0.310 ± 0.016	0.306 ± 0.010	0.3028 ± 0.0096	0.349 ± 0.041	0.314 ± 0.013	0.312 ± 0.013
H_0	67.71 ± 1.20	67.99 ± 0.79	68.22 ± 0.75	64.10 ± 3.26	66.99 ± 1.22	67.08 ± 1.21
$\chi^2_{min}/2$	4902.799	4904.074	4908.849	4902.921	4903.957	4908.846

(b) Mean values and 68% (or 95%) confidence limits for primary/derived parameters for a designer $f(R)$ model on a ΛCDM/wCDM background

	$f(R) + \Lambda$CDM			$f(R) + w$CDM		
	Planck $+$ WP	Planck $+$ WP $+$ BAO	Planck $+$ WP$+$ BAO $+$ lensing	Planck $+$ WP	Planck $+$ WP $+$ BAO	Planck $+$ WP$+$ BAO $+$ lensing
Parameters	mean $\pm$68% C.L.	mean $\pm$68% C.L.	mean $\pm$68% C.L.	mean $\pm$68% C.L.	mean $\pm$68% C.L.	mean $\pm$68% C.L.
$100\Omega_b h^2$	2.224 ± 0.033	2.220 ± 0.027	2.214 ± 0.025	2.255 ± 0.033	2.246 ± 0.029	2.226 ± 0.026
$\Omega_c h^2$	0.1185 ± 0.0027	0.1187 ± 0.0017	0.1184 ± 0.0016	0.1162 ± 0.0027	0.1174 ± 0.0019	0.1174 ± 0.0016
$100\theta_{MC}$	1.04149 ± 0.00067	1.04142 ± 0.00057	1.04136 ± 0.00056	1.04186 ± 0.00066	1.04166 ± 0.00060	1.04149 ± 0.00056
τ	0.088 ± 0.013	0.087 ± 0.013	0.087 ± 0.012	0.086 ± 0.013	0.084 ± 0.012	0.082 ± 0.012
n_s	0.9634 ± 0.0076	0.9624 ± 0.0058	0.9625 ± 0.0057	0.9695 ± 0.0078	0.9665 ± 0.0062	0.9647 ± 0.0057
$\log(10^{10}A_s)$	3.083 ± 0.025	3.082 ± 0.025	3.080 ± 0.022	3.075 ± 0.025	3.072 ± 0.024	3.067 ± 0.024
$\log_{10}B_0$	< 0.0 [a]	< 0.0 [a]	< -2.37 (95% C.L.)	$-1.97^{+1.61}_{-1.52}$ (95% C.L.)	$-2.01^{+1.60}_{-1.51}$ (95% C.L.)	$-3.35^{+1.79}_{-1.77}$ (95% C.L.)
w_0	$\cdots$	$\cdots$	$\cdots$	$(-1, -0.94)$ (95% C.L.)	$(-1, -0.94)$ (95% C.L.)	$(-1, -0.9997)$ (95% C.L.)
Ω_m	0.300 ± 0.017	0.302 ± 0.010	0.3005 ± 0.0092	0.291 ± 0.015	0.2982 ± 0.0099	0.2944 ± 0.0093
H_0	68.51 ± 1.30	68.35 ± 0.81	68.41 ± 0.72	69.04 ± 1.18	68.50 ± 0.80	68.89 ± 0.75
$\chi^2_{min}/2$	4900.765	4901.399	4907.901	4900.656	4901.140	4908.286

[a]No significant upper bound found in the parameter range we investigated.

do not find other remarkable degeneracies between B_0 and standard cosmological parameters.

V. CONCLUSIONS

Solving the puzzle of cosmic acceleration is one of the major challenges of modern cosmology. In this respect, cosmological surveys will provide a large amount of high-quality data, allowing for the testing of gravity on large scales with unprecedented accuracy. The effective field theory framework for cosmic acceleration will prove useful in performing model-independent tests of gravity and in testing specific theories, as (while being a parametrization of the quadratic action) it preserves a direct link to a wide range of DE/MG models. Indeed, any single-scalar-field DE/MG models with a well-defined Jordan frame can be cast into the EFT language and most of the cosmological models of interest fall into this class.

In a previous work [70], we presented the implementation of the EFT formalism into the Einstein-Boltzmann solver CAMB [71], resulting in EFTCAMB. The latter code has several virtues: it allows for the implementation of the

parametrized EFT framework in what we dub the pure EFT approach, and for the implementation of specific DE/MG models in the mapping mode; it does not rely on any quasistatic approximation, but rather it implements the full perturbative equations on all linear scales for both the pure and mapping cases, ensuring that no potentially interesting physics is lost; it has a built-in check of the stability conditions of perturbations in the dark sector in order to guarantee that the underlying gravitational theory is viable; and it enables one to choose among different expansion histories—namely, ΛCDM, wCDM, and CPL backgrounds—which naturally allows phantom-divide crossings.

In the present work, we equipped EFTCAMB with a modified version of CosmoMC, which we dubbed EFTCosmoMC, creating a bridge between the EFT parametrization of the dynamics of perturbations and observations. EFTCosmoMC allows one to practically perform tests of gravity and get constraints analyzing the cosmological parameter space with (in its current version) data sets, such as Planck, WP, BAO, and Planck lensing. Further data sets, mainly from large-scale structure surveys, will be included in the near future.

As discussed in Sec. III, exploring the parameter space requires a step-by-step check of the stability of the theory. We implemented the resulting stability conditions as viability priors that reject the Monte Carlo step whenever it falls in the unstable region of the parameter space. The latter procedure, in our view, represents a clean and natural way to impose priors on parameters describing the dark sector.

To illustrate the use of the EFTCAMB/EFTCosmoMC package, we have derived constraints on two different classes of models: a pure linear EFT model and a mapping designer $f(R)$. We used three different combinations of Planck, WP, BAO, and CMB lensing data sets to show their different effects on constraining the parameter space. For both models we have adopted the designer approach built in to EFTCAMB and have considered the case of a ΛCDM and a wCDM background.

For the linear EFT model, we have derived bounds on the only model parameter, i.e., the present value of the conformal coupling functions Ω_0^{EFT}, as described in Sec. IV B. In the case of a ΛCDM background, we have found that the latter needs to satisfy $\Omega_0^{\text{EFT}} \geq 0$ as a viability condition and with Planck + WP + BAO + lensing data we get a bound of $\Omega_0^{\text{EFT}} < 0.061$ (95% C.L.). (The three different data compilations give similar results.) For the wCDM expansion history, the outcome of the stability analysis is shown in Fig. 1; specifically, there is a stable region in parameter space where the dark energy equation of state can be smaller than -1 as long as the corresponding value of Ω_0^{EFT} is high enough to stabilize perturbations in the dark sector. Finally, the value $\Omega_0^{\text{EFT}} = 0$ corresponds to a minimally coupled model and requires $w_0 > -1$, as in the case of quintessence. The combined bound on Ω_0^{EFT} with Planck + WP + BAO + lensing data gives $\Omega_0^{\text{EFT}} < 0.058$ (95% C.L.).

Finally, we have investigated designer $f(R)$ models on ΛCDM/wCDM backgrounds, in terms of constraints on the model parameter B_0, as described in Sec. IV C. For the ΛCDM case we also compared our results to those that we obtained with the quasistatic treatment of these models via MGCAMB [102,103]. The two treatments give results that are in good agreement, with bounds from EFTCAMB/ EFTCosmoMC being a little tighter thanks to the full treatment of the dynamics of perturbations. On a wCDM background we have found a nontrivial likelihood profile of $\log_{10} B_0$ [see Fig. 3(d)] for all three data compilations and the shape of the marginalized posterior distribution in this case strongly reflects that of the viable region in parameter space. On the wCDM background, with Planck + WP + BAO + lensing data we get $\log_{10} B_0 = -3.35^{+1.79}_{-1.77}$ (95% C.L.). The bounds on w_0 with Planck lensing data [$w_0 \in (-1, -0.9997)$ (95% C.L.)] are quite stringent compared to those without this data set [$w_0 \in (-1, -0.94)$ (95% C.L.)] due to the high constraining power of lensing measurements on B_0 and the strong correlation between w_0 and B_0 via the viability prior.

Within the pure EFT approach, the code we are releasing already contains all operators relevant for the dynamics of linear perturbations. In particular, while in this work we showed results for a model involving only background operators, we shall stress that the code is fully functional for second-order operators too. In the future we will add some third-order operators to study mildly nonlinear scales. As for the mapping mode, the code currently allows for a *full* treatment of $f(R)$ models via a specific designer approach that can handle ΛCDM, wCDM, and CPL backgrounds. We will gradually implement the mapping procedure for many other single-scalar-field DE/MG models which are of relevance for cosmological tests. Finally, more data sets will be added to EFTCosmoMC, allowing one to test gravity with the most recent data releases, with a particular emphasis toward large-scale structure observations in view of surveys such as Euclid [51].

The complete EFTCAMB/EFTCosmoMC bundle is now publicly available at http://www.lorentz.leidenuniv.nl/ hu/codes/.

[1] E. Bertschinger, Astrophys. J. **648**, 797 (2006).
[2] E. V. Linder and R. N. Cahn, Astropart. Phys. **28**, 481 (2007).
[3] P. Zhang, M. Liguori, R. Bean, and S. Dodelson, Phys. Rev. Lett. **99**, 141302 (2007).
[4] W. Hu and I. Sawicki, Phys. Rev. D **76**, 104043 (2007).
[5] L. Amendola, M. Kunz, and D. Sapone, J. Cosmol. Astropart. Phys. 04 (2008) 013.
[6] E. Bertschinger and P. Zukin, Phys. Rev. D **78**, 024015 (2008).
[7] S. F. Daniel, R. R. Caldwell, A. Cooray, and A. Melchiorri, Phys. Rev. D **77**, 103513 (2008).
[8] Y.-S. Song and K. Koyama, J. Cosmol. Astropart. Phys. 01 (2009) 048.
[9] C. Skordis, Phys. Rev. D **79**, 123527 (2009).
[10] Y.-S. Song and O. Dore, J. Cosmol. Astropart. Phys. 03 (2009) 025.
[11] G.-B. Zhao, L. Pogosian, A. Silvestri, and J. Zylberberg, Phys. Rev. Lett. **103**, 241301 (2009).
[12] Y.-S. Song, L. Hollenstein, G. Caldera-Cabral, and K. Koyama, J. Cosmol. Astropart. Phys. 04 (2010) 018.
[13] S. F. Daniel, E. V. Linder, T. L. Smith, R. R. Caldwell, A. Cooray, A. Leauthaud, and L. Lombriser, Phys. Rev. D **81**, 123508 (2010).
[14] L. Pogosian, A. Silvestri, K. Koyama, and G.-B. Zhao, Phys. Rev. D **81**, 104023 (2010).
[15] R. Bean and M. Tangmatitham, Phys. Rev. D **81**, 083534 (2010).
[16] G.-B. Zhao, T. Giannantonio, L. Pogosian, A. Silvestri, D. J. Bacon, K. Koyama, R. C. Nichol, and Y.-S. Song, Phys. Rev. D **81**, 103510 (2010).
[17] J. Dossett, M. Ishak, J. Moldenhauer, Y. Gong, A. Wang, Y. Gong, and A. Wang, J. Cosmol. Astropart. Phys. 04 (2010) 022.
[18] S. A. Thomas, S. A. Appleby, and J. Weller, J. Cosmol. Astropart. Phys. 03 (2011) 036.
[19] T. Baker, P. G. Ferreira, C. Skordis, and J. Zuntz, Phys. Rev. D **84**, 124018 (2011).
[20] D. B. Thomas and C. R. Contaldi, J. Cosmol. Astropart. Phys. 12 (2011) 013.
[21] J. N. Dossett, M. Ishak, and J. Moldenhauer, Phys. Rev. D **84**, 123001 (2011).
[22] G.-B. Zhao, H. Li, E. V. Linder, K. Koyama, D. J. Bacon, and X. Zhang, Phys. Rev. D **85**, 123546 (2012).
[23] A. Hojjati, G.-B. Zhao, L. Pogosian, A. Silvestri, R. Crittenden, and K. Koyama, Phys. Rev. D **85**, 043508 (2012).
[24] P. Brax, A.-C. Davis, and B. Li, Phys. Lett. B **715**, 38 (2012).
[25] J. Dossett and M. Ishak, Phys. Rev. D **86**, 103008 (2012).
[26] P. Brax, A.-C. Davis, B. Li, and H. A. Winther, Phys. Rev. D **86**, 044015 (2012).
[27] I. Sawicki, I. D. Saltas, L. Amendola, and M. Kunz, J. Cosmol. Astropart. Phys. 01 (2013) 004.
[28] T. Baker, P. G. Ferreira, and C. Skordis, Phys. Rev. D **87**, 024015 (2013).
[29] L. Amendola, M. Kunz, M. Motta, I. D. Saltas, and I. Sawicki, Phys. Rev. D **87**, 023501 (2013).
[30] A. Hojjati, J. Cosmol. Astropart. Phys. 01 (2013) 009.

[31] A. Silvestri, L. Pogosian, and R. V. Buniy, Phys. Rev. D **87**, 104015 (2013).
[32] B. Hu, M. Liguori, N. Bartolo, and S. Matarrese, Phys. Rev. D **88**, 024012 (2013).
[33] J. Dossett and M. Ishak, Phys. Rev. D **88**, 103008 (2013).
[34] B. Hu, M. Liguori, N. Bartolo, and S. Matarrese, Phys. Rev. D **88**, 123514 (2013).
[35] M. Motta, I. Sawicki, I. D. Saltas, L. Amendola, and M. Kunz, Phys. Rev. D **88**, 124035 (2013).
[36] S. Asaba, C. Hikage, K. Koyama, G.-B. Zhao, A. Hojjati, and L. Pogosian, J. Cosmol. Astropart. Phys. 08 (2013) 029.
[37] A. Terukina, L. Lombriser, K. Yamamoto, D. Bacon, K. Koyama, and R. C. Nichol, J. Cosmol. Astropart. Phys. 04 (2014) 013.
[38] F. Piazza, H. Steigerwald, and C. Marinoni, J. Cosmol. Astropart. Phys. 05 (2014) 043.
[39] T. Baker, P. G. Ferreira, and C. Skordis, Phys. Rev. D **89**, 024026 (2014).
[40] Lás. Á.Gergely and S. Tsujikawa, Phys. Rev. D **89**, 064059 (2014).
[41] D. Munshi, B. Hu, A. Renzi, A. Heavens, and P. Coles, Mon. Not. R. Astron. Soc. **442**, 821 (2014).
[42] H. Steigerwald, J. Bel, and C. Marinoni, J. Cosmol. Astropart. Phys. 05 (2014) 042.
[43] Q.-G. Huang, arXiv:1403.0655 [Eur. Phys J. C (to be published)].
[44] L. Lombriser, arXiv:1403.4268.
[45] S. Tsujikawa, arXiv:1404.2684.
[46] E. Bellini and I. Sawicki, arXiv:1404.3713 [J. Cosmol. Astropart. Phys. (to be published)].
[47] http://www.sci.esa.int/planck.
[48] http://www.sdss.org.
[49] http://www.darkenergysurvey.org.
[50] http://www.lsst.org.
[51] http://www.sci.esa.int/euclid.
[52] M. J. Drinkwater et al., Mon. Not. R. Astron. Soc. **401**, 1429 (2010).
[53] D. Parkinson et al., Phys. Rev. D **86**, 103518 (2012).
[54] F. Simpson et al., arXiv:1212.3339 [Mon. Not. R. Astron. Soc. (to be published)].
[55] C. Heymans et al., arXiv:1303.1808.
[56] L. Fu et al., arXiv:1404.5469 [Mon. Not. R. Astron. Soc. (to be published)].
[57] G. Gubitosi, F. Piazza, and F. Vernizzi, J. Cosmol. Astropart. Phys. 02 (2013) 032.
[58] J. K. Bloomfield, É. É. Flanagan, M. Park, and S. Watson, J. Cosmol. Astropart. Phys. 08 (2013) 010.
[59] R. A. Battye and J. A. Pearson, J. Cosmol. Astropart. Phys. 07 (2012) 019.
[60] S. Weinberg, Phys. Rev. D **77**, 123541 (2008).
[61] P. Creminelli, G. D'Amico, J. Norena, and F. Vernizzi, J. Cosmol. Astropart. Phys. 02 (2009) 018.
[62] M. Park, K. M. Zurek, and S. Watson, Phys. Rev. D **81**, 124008 (2010).
[63] C. Cheung, A. Liam Fitzpatrick, J. Kaplan, L. Senatore, and P. Creminelli, J. High Energy Phys. 03 (2008) 014.
[64] R. Jimenez, P. Talavera, and L. Verde, Int. J. Mod. Phys. A **27**, 1250174 (2012).

[65] J. J. M. Carrasco, M. P. Hertzberg, and L. Senatore, J. High Energy Phys. 09 (2012) 082.

[66] M. P. Hertzberg, Phys. Rev. D **89,** 043521 (2014).

[67] J. Gleyzes, D. Langlois, F. Piazza, and F. Vernizzi, J. Cosmol. Astropart. Phys. 08 (2013) 025.

[68] J. Bloomfield, J. Cosmol. Astropart. Phys. 12 (2013) 044.

[69] F. Piazza and F. Vernizzi, Classical Quantum Gravity **30,** 214007 (2013).

[70] B. Hu, M. Raveri, N. Frusciante, and A. Silvestri, Phys. Rev. D **89,** 103530 (2014).

[71] http://www.camb.info.

[72] A. Lewis, A. Challinor, and A. Lasenby, Astrophys. J. **538,** 473 (2000).

[73] A. Lewis and S. Bridle, Phys. Rev. D **66,** 103511 (2002).

[74] M. Raveri, B. Hu, N. Frusciante, and A. Silvestri (to be published).

[75] G. W. Horndeski, Int. J. Theor. Phys. **10,** 363 (1974).

[76] E. J. Copeland, M. Sami, and S. Tsujikawa, Int. J. Mod. Phys. D **15,** 1753 (2006).

[77] C. Armendariz-Picon, T. Damour, and V. F. Mukhanov, Phys. Lett. B **458,** 209 (1999).

[78] C. Deffayet, G. Esposito-Farese, and A. Vikman, Phys. Rev. D **79,** 084003 (2009).

[79] A. Nicolis, R. Rattazzi, and E. Trincherini, Phys. Rev. D **79,** 064036 (2009).

[80] J. Bloomfield and J. Pearson, J. Cosmol. Astropart. Phys. 03 (2014) 017.

[81] R. A. Battye and J. A. Pearson, J. Cosmol. Astropart. Phys. 03 (2014) 051.

[82] N. Frusciante, M. Raveri, and A. Silvestri, J. Cosmol. Astropart. Phys. 02 (2014) 026.

[83] M. Chevallier and D. Polarski, Int. J. Mod. Phys. D **10,** 213 (2001).

[84] E. V. Linder, Phys. Rev. Lett. **90,** 091301 (2003).

[85] Y.-S. Song, W. Hu, and I. Sawicki, Phys. Rev. D **75,** 044004 (2007).

[86] L. Pogosian and A. Silvestri, Phys. Rev. D **77,** 023503 (2008); **81,** 049901(E) (2010).

[87] *Markov Chain Monte Carlo In Practice*, edited by W. R. Gilks, S. Richardson, and D. Spiegelhalter (Chapman and Hall/CRC, London, 1996).

[88] P. A. R. Ade *et al.* (Planck Collaboration), arXiv:1303.5075.

[89] P. A. R. Ade *et al.* (Planck Collaboration), arXiv: 1303.5076 [Astron. Astrophys. (to be published)].

[90] P. A. R. Ade *et al.* (Planck Collaboration), arXiv: 1303.5077.

[91] G. Hinshaw *et al.* (WMAP Collaboration), Astrophys. J. Suppl. Ser. **208,** 19 (2013).

[92] F. Beutler, C. Blake, M. Colless, D. Heath Jones, L. Staveley-Smith, L. Campbell, Q. Parker, W. Saunders, and F. Watson, Mon. Not. R. Astron. Soc. **416,** 3017 (2011).

[93] W. J. Percival *et al.* (SDSS Collaboration), Mon. Not. R. Astron. Soc. **401,** 2148 (2010).

[94] N. Padmanabhan, X. Xu, D. J. Eisenstein, R. Scalzo, A. J. Cuesta, K. T. Mehta, and E. Kazin, Mon. Not. R. Astron. Soc. **427,** 2132 (2012).

[95] L. Anderson *et al.*, Mon. Not. R. Astron. Soc. **427,** 3435 (2012).

[96] I. Zlatev, L.-M. Wang, and P. J. Steinhardt, Phys. Rev. Lett. **82,** 896 (1999).

[97] R. Bean, D. Bernat, L. Pogosian, A. Silvestri, and M. Trodden, Phys. Rev. D **75,** 064020 (2007).

[98] A. De Felice and S. Tsujikawa, Living Rev. Relativity **13,** 3 (2010).

[99] A. A. Starobinsky, JETP Lett. **86,** 157 (2007).

[100] L. Amendola, R. Gannouji, D. Polarski, and S. Tsujikawa, Phys. Rev. D **75,** 083504 (2007).

[101] W. Hu and I. Sawicki, Phys. Rev. D **76,** 064004 (2007).

[102] G.-B. Zhao, L. Pogosian, A. Silvestri, and J. Zylberberg, Phys. Rev. D **79,** 083513 (2009).

[103] A. Hojjati, L. Pogosian, and G.-B. Zhao, J. Cosmol. Astropart. Phys. 08 (2011) 005.

[104] A. Hojjati, L. Pogosian, A. Silvestri, and S. Talbot, Phys. Rev. D **86,** 123503 (2012).

[105] J. Dossett, B. Hu, and D. Parkinson, J. Cosmol. Astropart. Phys. 03 (2014) 046.